Numerical Methods in Civil Engineering, 7-1 (2022) 16-27

Numerical Methods in Civil Engineering

Journal Homepage: https://nmce.kntu.ac.ir/

Probabilistic performance assessment of seismically excited buildings with semi-active fluid viscous dampers

Ali Asghar Naderi*, Sina Bakhshinezhad and Shahrokh Rezaei*****

ARTICLE INFO

RESEARCH PAPER

Article history:
Received:
August 2021.
Revised:
May 2022.
Accepted:
May 2022.

Keywords:
Semi-active fluid viscous dampers, Probabilistic seismic performance assessment, Uncertain seismic demand, Fragility analysis, Ground-hook control, Sky-hook control

Abstract:

This paper presents a procedure to assess the probabilistic performance of the semi-active fluid viscous dampers (SAFVDs) utilized in seismically excited buildings. Some efficient on-off semi-active control algorithms based on motion towards or away from equilibrium, sky-hook, and ground-hook have been considered to determine the variable damping in each time step. The probabilistic relationship between intensity measure (IM) and seismic demand of the building has been estimated based on cloud analysis. A linear regression analysis has been employed to calculate the probabilistic demand parameters. A three-story nonlinear shear-type building equipped with SAFVDs has been adopted for the numerical example. The building has been subjected to a set of 20 actual earthquke records with the probability of occurrence of 10% in 50 years for the site of interest. The probabilistic performance of the nonlinear building equipped with SAFVDs has been assessed in terms of demand and fragility curves. The results indicate the effectiveness of the SAFVD systems in mitigating the fragility and enhancing the safety of the building. Particularly, a fragility reduction of about 51% is achieved at the immediate occupancy (IO) performance level using the SAFVD system.

1. Introduction

During past years, several energy dissipation devices have been extensively used to improve the behavior of new and existing buildings subjected to natural hazards such as earthquakes and wind. Among these devices, fluid viscous dampers (FVDs) have received much attention due to their capabilities and effectiveness and have been implemented in many actual buildings. Numerous studies have presented various design methodologies for fluid viscous dampers [1-4]. A concise review of most of the design methods proposed has been presented by De Domenico et al. [5]. Recently, the semi-active fluid viscous damper (SAFVD) with adjustable characteristics has been introduced as an alternative to the conventional passive FVDs [6].

** Corresponding Author: Professor Assistant, Mechanical Engineering Department, Imam Ali University, Tehran, Iran.* aa.naderi@modares.ac.ir
*** Ph.D., Faculty of Engineering, University of Mohaghegh Ardabili, Ardabil, Iran.*
**** Ph.D., Faculty of Engineering, University of Tehran, Tehran, Iran.*

The semi-active devices incorporate the advantages of passive and active control systems. The semi-active control can offer adaptability and variability during dynamic loads with only a small power source. Therefore, semi-active devices' benefit is that they do not have any potential to destabilize the building. The semi-active control of fluid viscous damper was first implemented by Kobori et al. [7,8]. Gavin and Aldemir [9] have investigated the performance of SAFVDs attached in low-rise base-isolated buildings and shown the effectiveness of this control system. Pourzeinali and Mousanejad [10] have assessed the application of SAFVDs in an asymmetric 3-D high-rise building. They have concluded that optimally designed SAFVDs can significantly reduce the torsional effects of the asymmetric building. The influence of SAFVDs utilized in a single-degree-of-freedom (SDOF) building, as well as a base-isolated SDOF building, has been studied by Oliveira et al. [11, 12]. Hazaveh et al. [13] have assessed the performance of SAFVDs in improving the seismic behavior of a wide range of SDOF structures with different natural periods.

Also, experimental verification of the seismic behavior of SAFVDs has been conducted [14], and a code-based design procedure for SAFVDs has been represented [15]. Previous studies focused on the performance assessment of SAFVDs have been performed in a deterministic framework. However, uncertainties in seismic excitation can remarkably diminish the effectiveness of energy dissipation devices, including SAFVDs. This issue necessitates the probabilistic methodologies to precisely assess the performance of the buildings equipped with control systems. Therefore, the probabilistic assessment of SAFVDs utilized in seismically excited buildings has been addressed in this paper.

Over the past decade, several studies have been conducted on probabilistic seismic assessment of buildings equipped with energy dissipation devices such as base isolation [16-20], tuned mass dampers [21-23], and magnetorheological dampers [24-27]. Many investigations in the literature have also focused on fluid viscous dampers due to their capabilities. Tubaldi et al. [28] have assessed the probabilistic performance of two adjacent buildings connected by linear and nonlinear fluid viscous dampers. A probabilistic design approach that considers the seismic uncertainties have been proposed by Tubaldi et al. [29] to design linear fluid viscous dampers. The uncertainties of damper properties and the earthquake uncertainties have been incorporated in the probabilistic performance assessment of linear buildings equipped with viscous dampers [30]. Altieri et al. [31] have introduced a reliability-based method for the optimal design of viscous dampers for seismic protection of seismic structures. Also, some similar studies have assessed the performance of passive FVDs in a probabilistic framework [32-35]. In the light of previous studies, the probabilistic performance assessment of semi-active fluid viscous dampers has not been performed previously and has been addressed in the present paper.

The rest of the paper is organized as follows: in Section 2, dynamic equations of the building equipped with semi-active fluid viscous dampers are presented; in Section 3, the adopted semi-active control algorithms are described; in Section 4, the probabilistic formulation to quantify uncertain demand and fragility are explained; in Section 5, numerical analysis has been applied on a nonlinear three-story case study building equipped with SAFVDs, followed by a discussion and conclusion.

2. Dynamic equations of the building equipped with SAFVDs

This paper adopts a nonlinear shear-type building with one degree of freedom per story as the building case study model. This model is a simplified generalization of realistic buildings and has been assumed to apply semi-active control and reduce computational effort, as followed in numerous studies concerning the performance of energy dissipation devices. Note that the presented method could be employed for more complex steel or concrete buildings in future studies. The schematic view of a nonlinear N-story shear-type building equipped with SAFVDs installed between all successive floors has been shown in Figure 1. The semi-active dampers have been attached in a horizontal position using Chevron bracings.

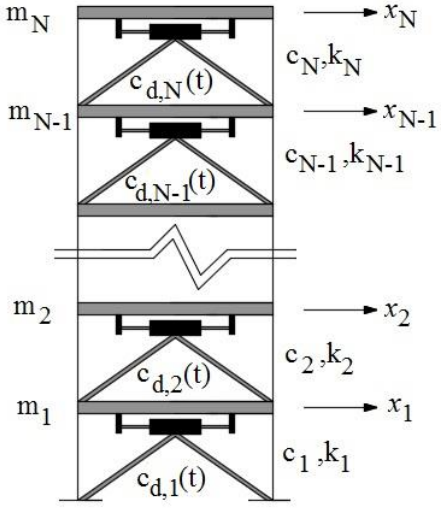

Fig. 1: Schematic view of the shear-type building equipped with SAFVDs

The dynamic equation of this nonlinear building subjected to ground acceleration $\ddot{x}_g$ is as:

$$\mathbf{M}\ddot{\mathbf{x}}(t)+\mathbf{f}_D\left(\dot{\mathbf{x}}(t)\right)+\mathbf{f}_S\left(\mathbf{x}(t)\right)=\mathbf{D}\mathbf{f}_d(t)+\mathbf{M}\mathbf{e}\ddot{x}_g(t) \qquad (1)$$

where $\mathbf{x}=[x_1,x_2,\dots,x_N]^T$ is the displacement response with respect to the ground, and the dots denote derivative with respect to time.

The vector $\mathbf{e}=[-1,\dots,-1]^T$ is the transformation vector of ground acceleration. By considering linear damping for the building, the damping force vector could be expressed as:

$$\mathbf{f}_D\left(\dot{\mathbf{x}}(t)\right)=\mathbf{C}\dot{\mathbf{x}}(t) \qquad (2)$$

where **C** is the damping matrix of the building, calculated by assuming a linear viscous damper for each story. The vector $\mathbf{F}_S$ is the restoring force vector and is a function of the displacement response of the building. It should be noted that the building, even controlled by energy dissipation devices, may undergo nonlinear behavior under seismic excitations, and thus, the nonlinearity of the structural behavior should be taken into account. It is noteworthy that the seismically excited buildings may experience inelastic behavior even when equipped with energy dissipation devices [36]. Therefore, it is more appropriate to account for the nonlinearity in the building's force-displacement relationship. In this paper, a bilinear hysteretic behavior has been adopted, as shown in Figure 2. This model is described

by the elastic stiffness K_E, post-elastic stiffness K_{PE}, and yielding drift u_y.

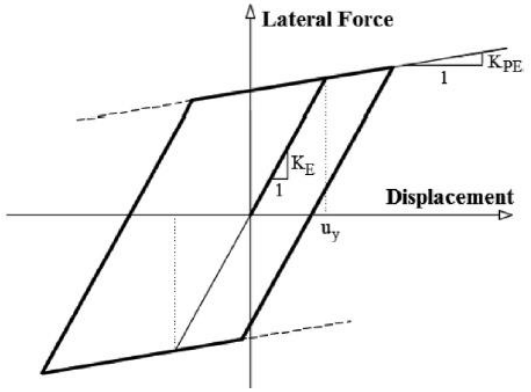

Fig. 2: Bilinear elastic-plastic stiffness model

By assuming that the dampers are installed in a horizontal position in all stories, the location matrix of dampers, **D**, is as follows:

$$\mathbf{D}=\begin{bmatrix} -1 & 1 & \text{L} & 0 & 0 \\ 0 & -1 & \text{L} & 0 & 0 \\ \text{M} & \text{O} & \text{O} & \text{M} & \text{M} \\ 0 & 0 & \text{O} & -1 & 1 \\ 0 & 0 & \text{L} & 0 & -1 \end{bmatrix} \tag{3}$$

$\mathbf{f}_d = [f_{d,1}, f_{d,2}, \ldots, f_{d,N}]^T$ is the vector of damper control force. Also, the damper force of the *i*th SAFVD could be expressed by:

$$f_{d,i}(t) = c_{d,i}(t) v_i^n(t) \qquad i = 1,2,...,N \tag{4}$$

where v_i is the relative velocity of the two ends of the *i*th damper. $c_{d,i}$ is the semi-active damping coefficient of the *i*th damper. n is the velocity exponent, which relates to the passing quality of the fluid and is usually between 0.15 and 1. This parameter describes the linear or nonlinear behavior of the damper. The velocity exponent equal to n=1 relates to the linear behavior of SAFVD, and the values lower than one (n<1) relate to nonlinear behavior.

In this study, SAFVDs with linear behavior have been considered.

3. semi-active control algorithm

The semi-active control of fluid viscous dampers offers the opportunity to meet the desired performance level for seismically excited buildings. In this paper, the efficiency of different control algorithms is investigated. Three main control algorithms have been considered, which are based on (1) motion towards or away from equilibrium, (2) sky-hook, and (3) ground-hook. All these algorithms control the opening and closing instant of the orifice of the semi-active device and hence switch the damper between the minimum and maximum damping in an on-off state. The control law and mathematic equations of these control algorithms have been described in the following sub-sections.

3.1 Motion towards or away from equilibrium

Hazaveh et al. [13] have proposed two semi-active control algorithms for the fluid viscous damper. Accordingly, the motion of the building is categorized into two states of motion toward equilibrium and motion away from equilibrium. The first control algorithm, which is called herein as "2-4 quarter", commands maximum damping when the motion is towards equilibrium. This control algorithm could be expressed by:

$$c_{d,i}(t) = \begin{cases} c_{d,\min} & if \quad Drift_i(t) \times V_i(t) \geq 0 \\ c_{d,\max} & if \quad Drift_i(t) \times V_i(t) < 0 \end{cases} \tag{5}$$

where i=1,2,…,N stands for the story number. *Drift* and *V* also denote the relative displacement and velocity of the story, respectively. Conversely, the second control algorithm, called "1-3 quarter", commands maximum damping when the motion is away from equilibrium and could be written as follows:

$$c_{d,i}(t) = \begin{cases} c_{d,\max} & if \quad Drift_i(t) \times V_i(t) \geq 0 \\ c_{d,\min} & if \quad Drift_i(t) \times V_i(t) < 0 \end{cases} \tag{6}$$

3.2 Ground-hook control algorithm

Ground-hook control is one of the most simple and effective control laws for semi-active damping control [37]. This control algorithm was first used in the suspension system of vehicles and then was utilized in structural control applications such as semi-active tuned mass dampers [38-40]. The ground-hook control algorithm comprises two laws; velocity-based ground-hook (VBG) and displacement-based ground-hook (DBG). The VBG control algorithm could be expressed as:

$$c_{d,i}(t) = \begin{cases} c_{d,\max} & if \quad \dot{x}_i(t) \times V_i(t) \geq 0 \\ c_{d,\min} & if \quad \dot{x}_i(t) \times V_i(t) < 0 \end{cases} \tag{7}$$

Contrarily, the DBG control algorithm is as follows:

$$c_{d,i}(t) = \begin{cases} c_{d,\max} & if \quad x_i(t) \times V_i(t) \geq 0 \\ c_{d,\min} & if \quad x_i(t) \times V_i(t) < 0 \end{cases} \tag{8}$$

3.3 Sky-hook control algorithm

The sky-hook control algorithm is another method that is similar to ground-hook control. This control law has been extensively employed in vehicle suspension systems [41]. The sky-hook control algorithm consists of two different

laws; velocity-based sky-hook (VBS) and displacement-based sky-hook (DBS). The VBS control law is as follows:

$$c_{d,i}(t)=\begin{cases} c_{d,\max} & if \quad \& \; x_{i+1}(t)\times V_i(t)\geq 0 \\ c_{d,\min} & if \quad \& \; x_{i+1}(t)\times V_i(t)<0 \end{cases} \tag{9}$$

Also, the DBS control algorithm is as follows:

$$c_{d,i}(t)=\begin{cases} c_{d,\max} & if \quad x_{i+1}(t)\times V_i(t)\geq 0 \\ c_{d,\min} & if \quad x_{i+1}(t)\times V_i(t)<0 \end{cases} \tag{10}$$

4. Probabilistic seismic assessment

The uncertainty in the applied seismic excitation is one of the most important issues in the performance assessment of seismically excited buildings. Indeed, the inherent randomness of earthquakes leads to uncertainty in the seismic demand of the building and may cause inefficiency in energy dissipation devices. Accordingly, accurate performance assessment of energy dissipation devices entails the adoption of a probabilistic framework. In this paper, a probabilistic approach has been utilized to estimate the uncertain engineering demand parameters (EDPs). Several methods have been established to represent a relationship between the intensity measure (IM) and seismic demand of the building, including incremental dynamic analysis [42], multiple strip analysis [43], and cloud analysis [44]. The cloud analysis benefits by not altering the frequency content of the earthquake records since the dynamic analyses are required only at the original scale of the earthquakes. Therefore, less dynamic analyses are also needed in this method. The cloud analysis has been proposed by Cornell et al. [44] and extensively employed in many probabilistic performance assessment studies similar to the work presented by Bakhshinezhad and Mohebbi [21]. According to the cloud analysis, the relationship between IM and EDP is expressed by the following power model:

$$EDP = a\, IM^{b} \tag{11}$$

where a and b are constants coefficients of the power model. The linear form of this equation could be obtained as the following by logarithmic transformation:

$$\ln(EDP)=\ln(a)+b\ln(IM) \tag{12}$$

To determine the constants a and b, first, a set of earthquake records should be selected, and the maximum building responses should be calculated by dynamic analysis under these earthquakes. Each response corresponds to a specific IM. Then, the constants a and b could be calculated using a linear regression analysis of ln(EDP) on ln(IM). The demand uncertainty or dispersion is obtained by:

$$\beta_{EDP|IM}=\sqrt{\ln(1+S^2)} \tag{13}$$

in which S^2 is the standard error as:

$$S^2=\sum\left(\ln(edp_i)-\ln(edp_p)\right)/n-2 \tag{14}$$

where edp_i and edp_p are the observed and predicted demand of the structure, respectively. The parameter n is the number of response sample data. The fragility function could be expressed by the following:

$$fragility=\Phi\left[\frac{\ln(EDP)-\ln(DM)}{\sqrt{\beta^2_{EDP|IM}+\beta^2_{DM}+\beta^2_{M}}}\right] \tag{15}$$

where Φ denotes the standard normal cumulative distribution function. β_M is the modeling uncertainty, for which the value of 0.3 has been considered according to Taylor [45]. DM and β_{DM} are damage measure capacity and damage measure uncertainty, respectively, addressed in the following sub-section.

4.1 Capacity and uncertainty of damage measures

The evaluation of the probabilistic performance of a building entails selecting appropriate damage measures. The inter-story drift ratio, as a safety criterion, has been employed as a global EDP that correlates with the damage to structural components. The damage measure capacities of inter-story drift ratio associated with steel moment frames have been assigned the values of 0.7%, 2.5%, and 5% [46] related to immediate occupancy (IO), life safety (LS), and collapse prevention (CP) performance levels, respectively. The damage measure uncertainty, β_{DM}, has been assigned the value of 0.3 for all performance levels, as suggested by Taylor [45].

5. Numerical analysis and discussion

In this section, the methodology of probabilistic performance assessment of semi-active fluid viscous dampers for seismically excited buildings has been explained through numerical analysis. The semi-active control of fluid viscous dampers has been performed through different on-off control algorithms such as motion towards or away from equilibrium, sky-hook, and ground-hook control algorithms. A linear SAFVD device has been attached to the first floor of the building, and nonlinear dynamic analyses have been conducted under a set of 20 actual earthquakes. It should be noted that the performance of the SAFVD system will be more effective if SAFVDs are installed in all stories. However, in this paper, the SAFVD device is only considered in the first story to investigate its effectiveness through a probabilistic framework. A

nonlinear three-story shear-type building with bilinear hysteretic material behavior has been considered as the case study building. The mass is 3.83 tons for all stories. The damping matrix has been determined by assuming the 2% damping for each floor. The elastic stiffness is 1550, 1960, and 1610 kN/m for the first to the third story. The ratio of post elastic stiffness to the elastic stiffness is K_{PE}/K_E=0.02, which is identical for all stories. Also, the yielding drift of each story is 5 cm. The fundamental period of the building based on its initial stiffness is T_1=0.67 sec. It should be noted that this shear building has been considered as a sample case study building following [47], while the applied probabilistic assessment method could be employed for more complex structures.

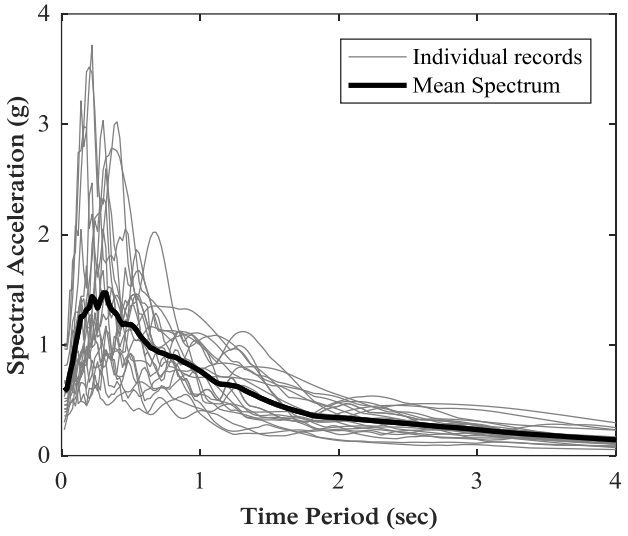

Fig. 3: Acceleration response spectrum of the selected earthquake records and the mean acceleration response spectrum

5.1 Earthquake ground motions set used in this study

The selection and number of earthquake records is an important issue in the probabilistic performance assessment of seismically excited buildings. Indeed, it is more appropriate to select a set of different earthquakes with different characteristics to take into account the record-to-record variability [48]. Regarding the number of records, applying seven pairs of earthquakes would be sufficient to estimate the structural responses accurately [49]. In this paper, a set of 10 pairs of earthquakes with the probability of occurrence of 10% in 50 years proposed for the SAC project for the Los Angeles area have been used for performance analysis. These earthquakes have different frequency contents, intensities, and durations to represent the variability of the seismic source. These earthquakes are within moderate to severe intensities. It should be noted that selecting earthquakes with small intensity without scaling does not have the proper intensity for LS or CP performance levels. Table 1 represents the properties of the selected earthquake records. The acceleration response spectrum of the selected earthquakes and the mean spectrum for 5% critical damping have shown in Figure 3.

Table 1: Selected earthquakes records used in this study

Earthquake code	Earthquake name	Station	PGA (g)	S_a (g)
La01	Imperial Valley-f_n	El Centro	0.46	0.61
La02	Imperial Valley-f_p	El Centro	0.68	1.33
La03	Imperial Valley-f_n	Array #05	0.39	0.92
La04	Imperial Valley-f_p	Array #05	0.49	0.53
La05	Imperial Valley-f_n	Array #06	0.30	0.51
La06	Imperial Valley-f_p	Array #06	0.23	0.47
La07	Landers-f_n	Barstow	0.42	0.63
La08	Landers-f_p	Barstow	0.43	0.95
La09	Landers-f_n	Yermo	0.52	1.25
La10	Landers-f_p	Yermo	0.36	0.96
La11	Loma Prieta-f_n	Gilroy	0.67	0.75
La12	Loma Prieta-f_p	Gilroy	0.97	0.74
La13	Northridge-f_n	Newhall	0.68	1.10
La14	Northridge-f_p	Newhall	0.66	1.22
La15	Northridge-f_n	Rinaldi RS	0.53	1.25
La16	Northridge-f_p	Rinaldi RS	0.58	1.45
La17	Northridge-f_n	Sylmar	0.57	0.65
La18	Northridge-f_p	Sylmar	0.82	0.86
La19	North Palm Springs-f_n	-	1.02	0.98
La20	North Palm Springs-f_p	-	0.99	1.23

5.2 Seismic performance of the SAFVD system

In this section, the seismic performance of the SAFVD systems has been assessed and compared with that of an uncontrolled structure. Six different on-off control algorithms based on motion towards or away from equilibrium, ground-hook, and sky-hook strategies, as discussed in Section 3, have been employed. A nonlinear three-story shear building equipped with a SAFVD in the first story has been adopted to assess the effectiveness of the control system. The semi-active device could be instantaneously switched between the minimum and maximum damping levels, which should be determined by the manufacturers according to the practical limitations of the device. As a sample, the minimum and maximum damping levels have been considered to have the values of 100 and 500 kN.s/m, respectively, which seems to be within the practical limits. It should be noted that these values have been considered as an example to explain the probabilistic performance assessment procedure of the semi-active dampers and could be designed optimally in further studies. The mean responses subjected to the 20 earthquake records for the uncontrolled building and the building equipped with

SAFVDs considering different control algorithms have been compared in Table 2. It seems that the SAFVDs have the capability of reducing the maximum drift and base shear responses significantly with respect to the uncontrolled structure using all control algorithms. Therefore, the SAFVD systems can effectively enhance the safety of the building since these responses are highly correlated with damage to structural elements.

The absolute acceleration response is also of interest due to relation to the occupants' convenience as well as the safety of non-structural components. Note that the acceleration amplification observed in other control algorithms may be due to instant switching of the semi-active damping and exerting an immediate impact on the building. Although some control algorithms seem inefficient in reducing this response, the 2-4 quarter and VBG show effective mitigation in the absolute acceleration of the building. For example, the SAFVD system based on the 2-4 quarter control algorithm has reduced the mean of maximum drift, absolute acceleration, and base shear by nearly 66%, 15%, and 39% with respect to the uncontrolled building. These response mitigations are also about 64%, 16%, and 67% for the VBG control algorithm.

Table 2: The mean responses of the uncontrolled building and the one equipped with SAFVDs based on different control strategies

Mechanism	Maximum drift (cm)	Maximum absolute acceleration (cm/s^2)	Maximum base shear (kN)
Uncontrolled	10.0	1413	77.2
2-4 quarter	3.44	1200	47.4
1-3 quarter	3.87	3567	32.1
VBG	3.62	1180	25.8
DBG	3.87	3567	32.1
VBS	3.37	2170	34.3
DBS	3.80	2871	29.2

The maximum drift and absolute acceleration over all stories of the uncontrolled building and the one equipped with SAFVDs based on the 2-4 quarter and VBG control algorithm subjected to 20 earthquakes have been compared in Figures 4 to 9. The mean responses for each story have also been shown in these figures. It appears that the SAFVD systems have reduced the maximum drift under all earthquakes with respect to the uncontrolled building. On the other hand, the SAFVDs, aside from a few records, have mitigated the maximum absolute acceleration under the majority of earthquakes. To compare the dispersion of the drift response, the standard deviation of the first story drift of the uncontrolled structure under 20 earthquakes is about 5.5 cm, while this standard deviation is reduced to 1.1 cm using the SAFVD based on the 2-4 quarter controller and also it is reduced to 0.47 cm based on the VBG controller. In addition, it could be stated that the semi-active damper system could effectively improve the seismic performance of the building, considering the safety of the entire building, the safety of non-structural components, and the convenience of occupants.

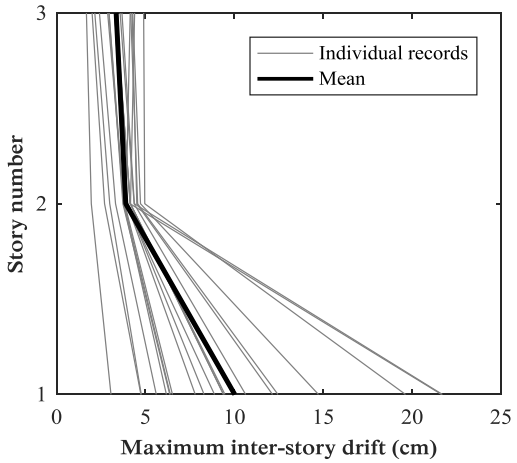

Fig. 4: Maximum drift of the uncontrolled building under each earthquake

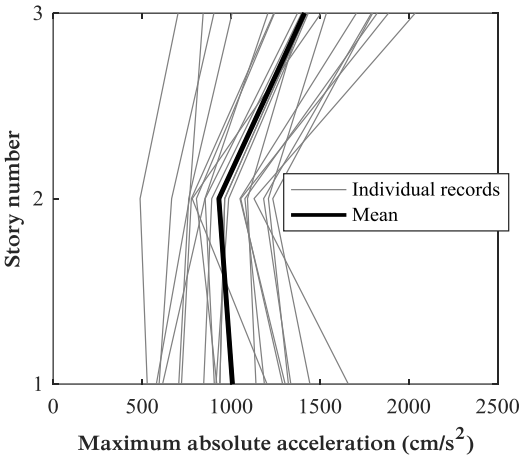

Fig. 5: Maximum absolute acceleration of the uncontrolled building under each earthquake

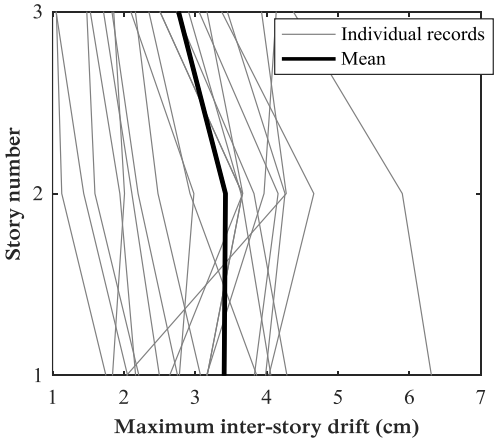

Fig. 6: Maximum drift of the building equipped with the SAFVD using the 2-4 quarter controller under each earthquake

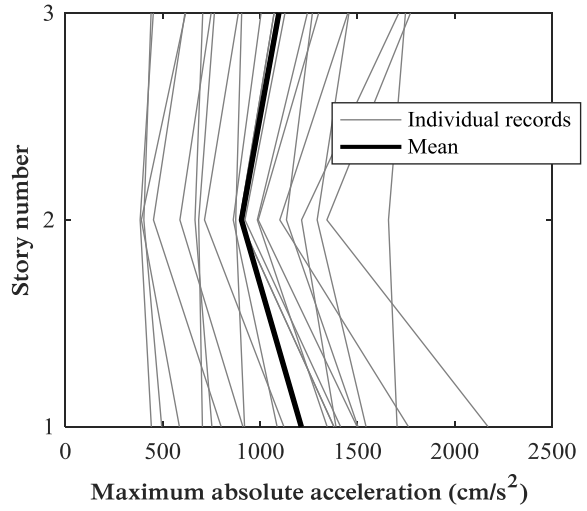

Fig. 7: Maximum absolute acceleration of the building equipped with the SAFVD using the 2-4 quarter controller under each earthquake

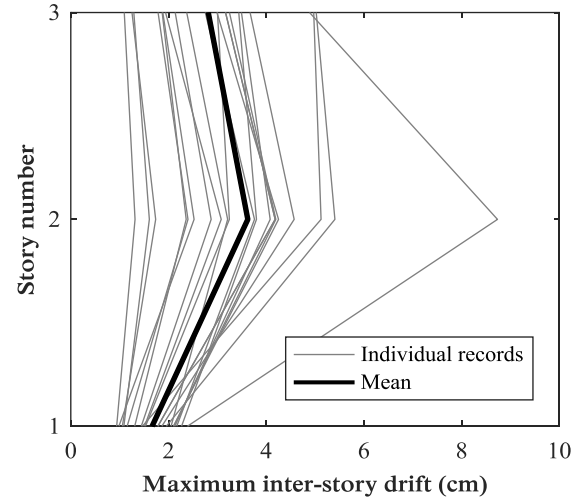

Fig. 8: Maximum drift of the building equipped with the SAFVD using the VBG controller under each earthquake

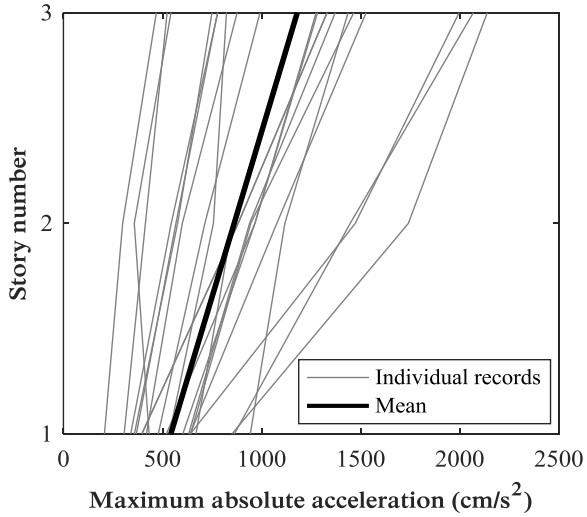

Fig. 9: Maximum absolute acceleration of the building equipped with the SAFVD using the VBG controller under each earthquake

As an example, the time histories of building story drift associated with the uncontrolled building and the building equipped with SAFVD system based on the 2-4 quarter control algorithm under earthquake number 11 have been compared in Figure 10. It is evident that the semi-active system kept the story drift within the elastic range and thus can protect the structural components. Also, Figure 11 shows the time histories of building story absolute acceleration for the controlled and uncontrolled buildings under this earthquake. It seems that the SAFVD can mitigate acceleration, especially after the first strikes of the earthquake, which can improve occupants' convenience and safety of non-structural components.

The time histories of the semi-active variable damping and the damper force of the SAFVD based on the 2-4 quarter control algorithm under earthquake number 11 have been illustrated in Figure 12. The instant switch between the minimum and maximum damping values of the SAFVD, which are 100 kN.s/m and 500 kN.s/m, respectively, is evident in this figure. Also, Figure 13 shows the hysteresis loops of the first story of the uncontrolled building and building equipped with SAFVD under this earthquake, indicating the semi-active system's effectiveness in seismic energy dissipation.

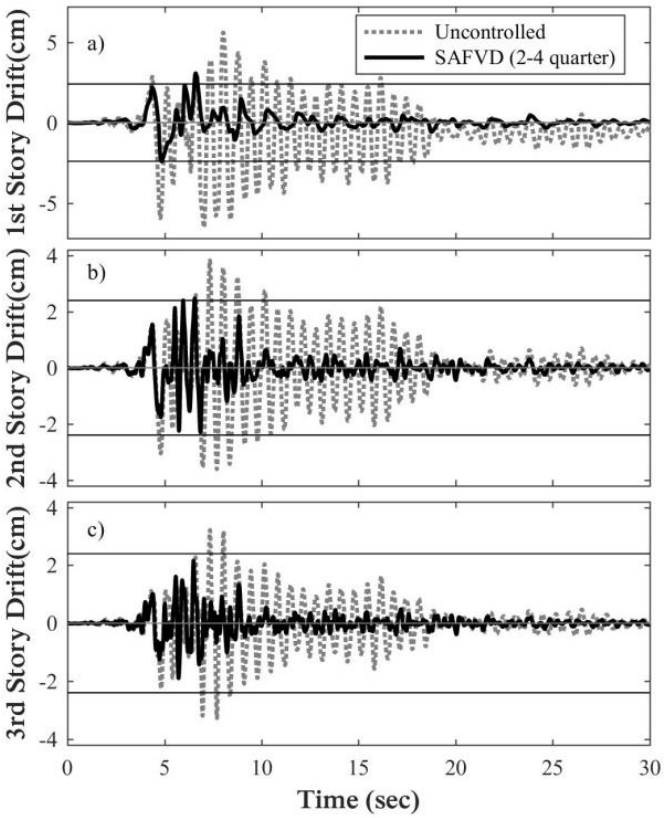

Fig. 10: Time histories of a) first story, b) second story, and c) third story drift of the uncontrolled building and building equipped with the SAFVD based on the 2-4 quarter control algorithm

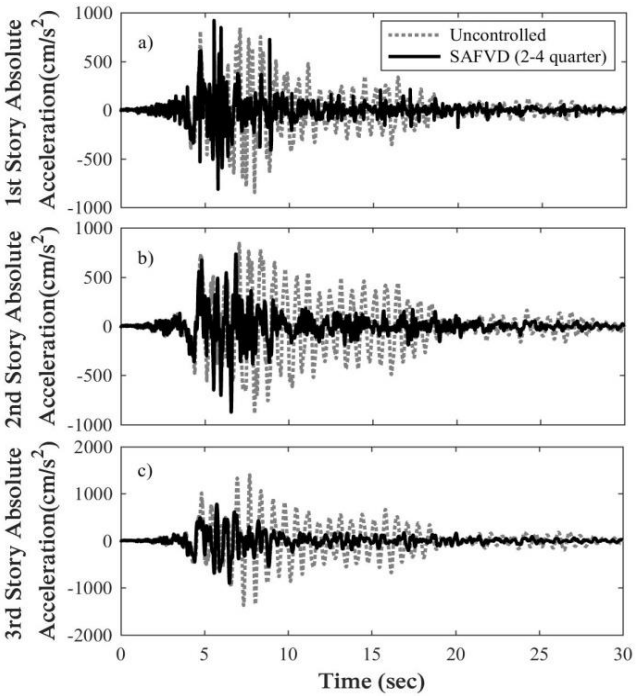

Fig. 11: Time histories of a) first story, b) second story, and c) third story absolute acceleration of the uncontrolled building and the building equipped with the SAFVD based on the 2-4 quarter control algorithm

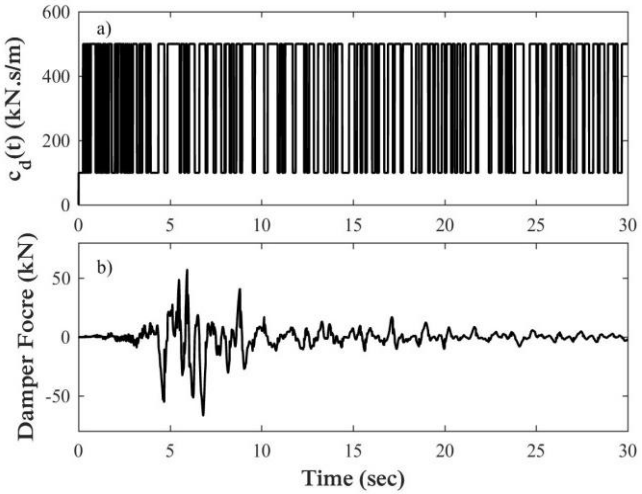

Fig. 12: Time histories of a) semi-active damping and b) damper force of the SAFVD based on the 2-4 quarter control algorithm

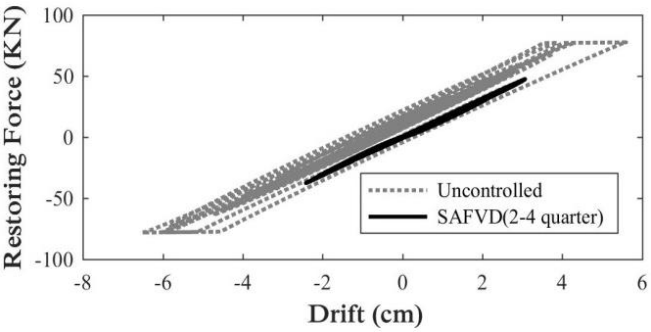

Fig. 13: Hysteresis loops of the first story of the uncontrolled building and the building equipped with SAFVD based on the 2-4 quarter control algorithm

5.3 Determining probabilistic parameters using regression analysis

In this section, the probabilistic parameters of the seismic building demand presented in Equation (11) have been derived using regression analysis. These parameters include *a*, *b*, and $\beta_{EDP|IM}$. The building has been subjected to 20 earthquakes, and the maximum drifts have been derived previously. The spectral acceleration at the fundamental period and damping ratio of the building, $S_a(T_1,\xi=2\%)$, has been selected as the IM. This IM has been proved to provide the sufficiency criteria [50]. The maximum drifts versus the S_a of the records have been considered as samples for the regression analysis. As mentioned before, the relationship between the natural logarithm of the maximum drift and the natural logarithm of S_a would be linear. Therefore, linear regression has been conducted to determine the properties of the line, such as slope, intercept, and correlation. As an example, the result of this analysis for the uncontrolled building is illustrated in Figure 14. The parameters *a* and *b* could be calculated based on the slope and y-intercept of the line according to Equation (12). Then the demand uncertainty, $\beta_{EDP|IM}$, is calculated by comparing the estimated and predicted responses using Equation (13).

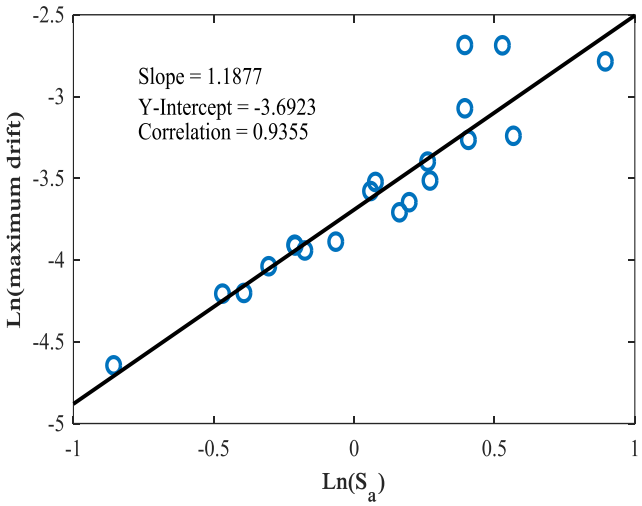

Fig. 14: The relationship between the demand and IM for the uncontrolled building

Table 3 reports the probabilistic parameters of a, b, and $\beta_{EDP|IM}$ related to the uncontrolled building and the building equipped with SAFVDs based on the 2-4 quarter and VBG control algorithms. These parameters have been employed to determine the uncertain demand and fragility, as discussed in the following section. It is noteworthy that the inter-story drift ratio has been considered as the failure criteria for the safety of structural components following the FEMA 356 [46] guidelines. The acceleration response could also be used as the failure criteria of non-structural components in further studies.

Table 3: Estimated probabilistic parameters of the uncontrolled building and the building equipped with SAFVDs

Mechanism	*a*	*b*	$\beta_{EDP\|IM}$
Uncontrolled	0.0249	1.1877	0.1905
2-4 quarter	0.0097	0.6191	0.1613
VBG	0.0097	0.7749	0.1658

5.4 Probabilistic seismic demand and fragility of SAFVD systems

This section assesses the probabilistic performance of the SAFVD system in terms of the probabilistic demand and fragility curves. Figure 15 shows the maximum drift demand curve of the uncontrolled building and the building equipped with SAFVDs based on the 2-4 quarter and VBG control algorithms. It is evident that the semi-active dampers can significantly mitigate the uncertain drift demand of the building, with the 2-4 quarter algorithm being more effective.

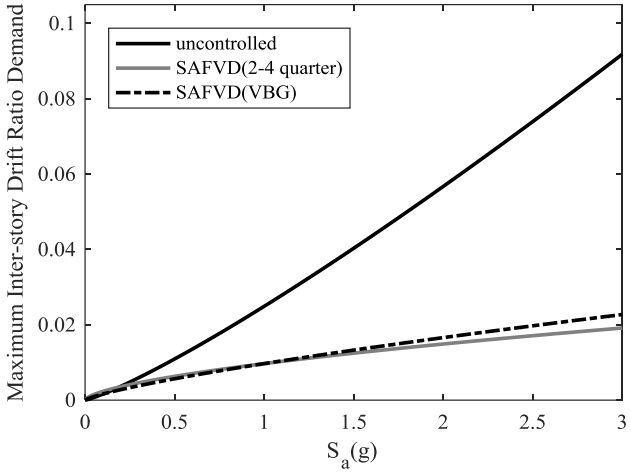

Fig. 15: The maximum drift demand curves of the uncontrolled building and the building equipped with SAFVDs

Furthermore, the corresponding fragility curves of the IO, LS, and CP performance levels are also compared in Figures. 16 to 18. It is observed that the SAFVDs are still effective in reducing the fragility of the building and hence improve the building's safety. Comparing the control algorithms, it seems both the control algorithms perform similarly at the IO performance level. As an example, the SAFVD based on the 2-4 quarter control algorithm has reduced the fragility by about 42% with respect to the uncontrolled building at the IO performance level and S_a=0.5g, while this fragility mitigation was about 51% for the VBG control algorithm.

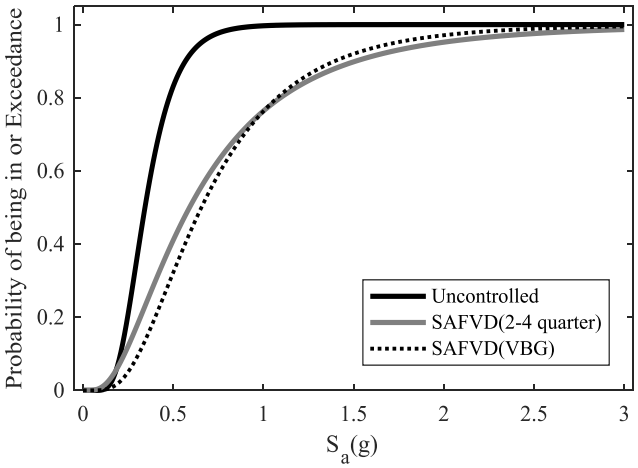

Fig. 16: Fragility curves of the uncontrolled building and building equipped with SAFVDs at the IO performance level

At higher performance levels, including LS and CP, the 2-4 quarter control algorithm shows more reduction in fragility, especially in higher S_a. As an example, the SAFVDs based on the VBG and 2-4 quarter control algorithms have shown similar performance and reduced the fragility at the LS performance level and S_a=1.0g by about 63%. In addition, it could be concluded that semi-active control of fluid viscous damper can enhance the probabilistic performance of the building significantly. It should be noted that these results have been derived for the considered case study building in the specific seismicity of the site (i.e., $S_a(T_1,\xi=2\%)$), and justification for SAFVDs entails further studies for different seismicity characteristics such as regions with a high frequency of small to medium earthquakes.

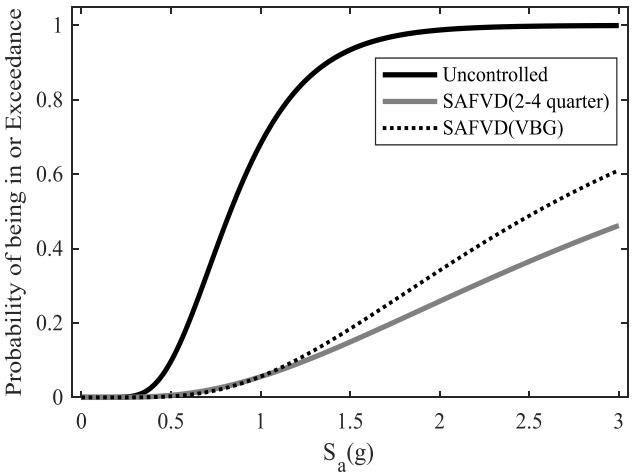

Fig. 17: Fragility curves of the uncontrolled building and the building equipped with SAFVDs at the LS performance level

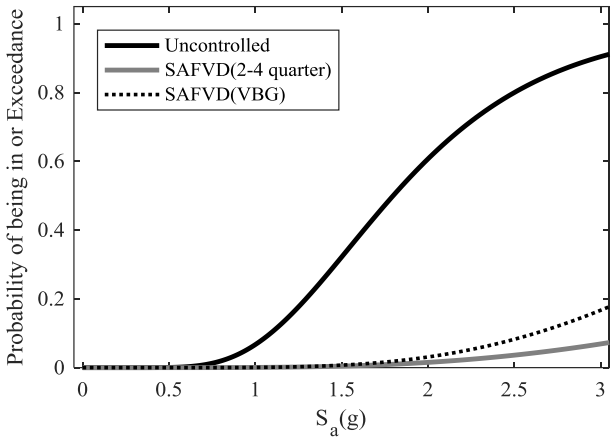

Fig. 18: Fragility curves of the uncontrolled building and the building equipped with SAFVDs at the CP performance level

6. Conclusions

In this study, it has been aimed to present a procedure to assess the probabilistic performance of the semi-active fluid viscous dampers, SAFVDs, attached to seismically excited buildings. Six on-off control algorithms based on the motion towards or away from equilibrium, sky-hook, and ground-hook have been employed to control the semi-active dampers. A three-story nonlinear shear building with bilinear hysteretic material behavior equipped with SAFVDs in the first story has been adopted, and nonlinear dynamic analyses have been conducted under 20 actual earthquakes. The cloud analysis and the regression analysis have been employed to estimate the relationship between intensity measure and seismic demand and probabilistic parameters of the demand. The numerical analyses illustrate the effectiveness of the semi-active control system in reducing the structural responses. The semi-active control algorithms based on motion towards equilibrium, i.e., the so-called "2-4 quarter" and velocity-based ground-hook algorithms, have shown to be the most effective. It is observed that SAFVDs based on both of these control algorithms significantly diminished the maximum drift, which enhances the safety of structural components. Also, these SAFVDs have effectively reduced the maximum absolute acceleration, which is the criterion of the convenience of occupants and the safety of non-structural components. As an example, the SAFVD based on the VBG control algorithm has reduced the mean of maximum drift and absolute acceleration by approximately 64% and 67%, respectively. On the other hand, the probabilistic performance of SAFVD systems has been assessed in terms of the seismic demand and fragility curves. These curves qualitatively illustrate the semi-active dampers' effectiveness in mitigating seismic demand and fragility and hence improving the safety of the building. In particular, the SAFVDs based on the velocity-based ground-hook control algorithm have reduced the seismic fragility by about 51% at the IO performance level and spectral acceleration of 0.3g.

References

[1] Shariati, A., Kamgar, R., & Rahgozar, R. (2020). Optimum Layout of Nonlinear Fluid Viscous Damper for Improvement the Responses of Tall Buildings. Optimization in Civil Engineering, 10(3), 411- 431.

[2] Hashemi, M. R., Vahdani, R., Gerami, M., & Kheyrodin, A. (2020). Viscous Damper Placement Optimization in Concrete Structures Using Colliding Bodies Algorithm and Story Damage Index. Optimization in Civil Engineering, 10(1), 53-70.

[3] Moradpour, S., & Dehestani, M. (2019). Optimal DDBD Procedure for Designing Steel Structures with Nonlinear Fluid Viscous Dampers. Structures, 22, 154-174.

[4] Idels, O., & Lavan, O. (2021). Optimization-based Seismic Design of Steel Moment-resisting Frames with Nonlinear Viscous Dampers. Structural Control and Health Monitoring, 28(1), Article e2655.

[5] De Domenico, D., Ricciardi, G., & Takewaki, I. (2019). Design Strategies of Viscous Dampers for Seismic Protection of Building Structures: a Review. Soil Dynamics and Earthquake Engineering, 118, 144-165.

[6] Symans, M. D., Constantinou, M. C. (1995). Development and Experimental Study of Semi-active Fluid Damping Devices for Seismic Protection of Structures (No.NCEER-95-0011). National Center for Earthquake Engineering Research.

[7] Kobori, T., Takahashi, M., Nasu, T., Niwa, N., & Ogasawara, K. (1993). Seismic Response Controlled Structure with Active Variable Stiffness System. Earthquake Engineering & Structural Dynamics, 22(11), 925-941.

[8] Kurata, N., Kobori, T., Takahashi, M., Niwa, N., & Midorikawa, H. (1999). Actual Seismic Response Controlled Building with Semi-active Damper System. Earthquake Engineering & Structural Dynamics, 28(11), 1427-1447.

[9] Gavin, H. P., & Aldemir, U. (2005). Optimal Control of Earthquake Response Using Semiactive Isolation. Engineering Mechanics, 131(8), 769-776.

[10] Pourzeynali, S., & Mousanejad, T. (2010). Optimization of Semi-active Control of Seismically Excited Buildings Using Genetic Algorithms. Scientia Iranica, 17(1), 26-38.

[11] Oliveira, F., Botto, M. A., Suleman, & A., Morais, P. (2012, July). Semi-active Viscous Damper for Controlling Civil Engineering Structures Subjected to Earthquakes. 10th Portuguese Conference on Automatic Control, Funchal, Portugal.

[12] Oliveira, F., Morais, P., & Suleman, A. (2012, September) Semi-active Control of a Fluid Viscous Damper for Vibration Mitigation. 15th World Conference on Earthquake Engineering, Lisbon, Portugal.

[13] Hazaveh, N. K., Rodgers, G. W., Chase, J. G., & Pampanin, S. (2017). Reshaping Structural Hysteresis Response with Semi-

active Viscous Damping. Bulletin of Earthquake Engineering, 15(4), 1789-1806.

[14] Hazaveh, N. K., Rodgers, G. W., Chase, J. G., & Pampanin, S. (2017). Experimental Test and Validation of a Direction-and Displacement-Dependent Viscous Damper. Engineering Mechanics, 143(11), Article e04017132.

[15] Hazaveh, N., Rodgers, G. W., Pampanin, S., & Chase, J. G. (2016). Damping Reduction Factors and Code-based Design Equation for Structures Using Semi-active Viscous Dampers. Earthquake Engineering & Structural Dynamics, 45(15), 2533-2550.

[16] Cardone, D., Perrone, G., & Piesco, V. (2019). Developing Collapse Fragility Curves for Base-isolated Buildings. Earthquake Engineering & Structural Dynamics, 48(1), 78-102.

[17] Shoaei, P., Orimi, H. T., & Zahrai, S. M. (2018). Seismic Reliability-based Design of Inelastic Base-isolated Structures with Lead-rubber Bearing Systems. Soil Dynamics and Earthquake Engineering, 115, 589-605.

[18] Castaldo, P., Amendola, G., & Palazzo, B. (2017). Seismic Fragility and Reliability of Structures Isolated by Friction Pendulum Devices: Seismic Reliability-based Design (SRBD). Earthquake Engineering & Structural Dynamics, 46(3), 425-446.

[19] Khansefid, A., Maghsoudi-Barmi, A., & Khaloo, A. (2019). Seismic Protection of LNG Tanks with Reliability Based Optimally Designed Combined Rubber Isolator and Friction Damper. Earthquakes and Structures, 16(5), 523-532.

[20] Öncü-Davas, S., & Alhan, C. (2019). Probabilistic Behavior of Semi-active Isolated Buildings under Pulse-like Earthquakes. Smart Structures and Systems. 23(3), 227-242.

[21] Bakhshinezhad, S., & Mohebbi, M. (2021). Multiple Failure Function Based Fragility Curves for Structures Equipped with TMD. Earthquake Engineering and Engineering Vibration, 20(2), 471-482.

[22] Bakhshinezhad, S., & Mohebbi, M. (2019). Multiple Failure Criteria-based Fragility Curves for Structures Equipped with SATMDs. Earthquakes and Structures, 17(5), 463-475.

[23] Bakhshinezhad, S., & Mohebbi, M. (2019). Fragility Curves for Structures Equipped with Optimal SATMDs. Optimization in Civil Engineering, 9(3), 437-455.

[24] Mohebbi, M., & Bakhshinezhad, S. (2021). Multiple Performance Criteria-based Risk Assessment for Structures Equipped with MR Dampers. Earthquakes and Structures, 20(5), 495-512.

[25] Hadidi, A., Azar, B. F., & Shirgir, S. (2019). Reliability Assessment of Semi-active Control of Structures with MR Damper. Earthquakes and Structures, 17(2), 131-141.

[26] Cha, Y. J., & Bai, J. W. (2016). Seismic Fragility Estimates of a Moment-resisting Frame Building Controlled by MR Dampers Using Performance-based Design. Engineering Structures, 116, 192-202.

[27] Bagherkhani, A., & Baghlani, A. (2021). Reliability Assessment of MR Fluid Dampers in Passive and Semi-active Seismic Control of Structures. Probabilistic Engineering Mechanics, 63, Article e103114.

[28] Tubaldi, E., Barbato, M., & Dall'Asta, A. (2014). Performance-based Seismic Risk Assessment for Buildings Equipped with Linear and Nonlinear Viscous Dampers. Engineering Structures, 78, 90-99.

[29] Tubaldi, E., Barbato, M., & Dall'Asta, A. (2016). Efficient Approach for the Reliability-based Design of Linear Damping Devices for Seismic Protection of Buildings. ASCE-ASME Journal of Risk and Uncertainty in Engineering Systems, Part A: Civil Engineering, 2(2), c4015009.

[30] Dall'Asta, A., Scozzese, F., Ragni, L., & Tubaldi, E. (2017). Effect of the Damper Property Variability on the Seismic Reliability of Linear Systems Equipped with Viscous Dampers. Bulletin of Earthquake Engineering, 15(11), 5025-5053.

[31] Altieri, D., Tubaldi, E., De Angelis, M., Patelli, E., & Dall'Asta, A. (2018). Reliability-based Optimal Design of Nonlinear Viscous Dampers for the Seismic Protection of Structural Systems. Bulletin of Earthquake Engineering, 16(2), 963-982.

[32] Dall′ Asta, A., Tubaldi, E., & Ragni, L. (2016). Influence of the Nonlinear Behavior of Viscous Dampers on the Seismic Demand Hazard of Building Frames. Earthquake Engineering & Structural Dynamics, 45(1), 149-169.

[33] Güneyisi, E. M., & Altay, G. (2008). Seismic Fragility Assessment of Effectiveness of Viscous Dampers in R/C Buildings Under Scenario Earthquakes. Structural Safety, 30(5), 461-480.

[34] Lavan, O., & Avishur, M. (2013). Seismic Behavior of Viscously Damped Yielding Frames Under Structural and Damping Uncertainties. Bulletin of Earthquake Engineering, 11(6), 2309-2332.

[35] Scozzese, F., Gioiella, L., Dall'Asta, A., Ragni, L., & Tubaldi, E. (2021). Influence of Viscous Dampers Ultimate Capacity on the Seismic Reliability of Building Structures. Structural Safety, 91, Article e102096.

[36] Khansefid, A., & Ahmadizadeh, M. (2016). An Investigation of the Effects of Structural Nonlinearity on the Seismic Performance Degradation of Active and Passive Control Systems Used for Supplemental Energy Dissipation. Vibration and Control, 22(16), 3544-3554.

[37] Valášek, M., Novak, M., Šika, Z., & Vaculin, O. (1997). Extended Ground-hook-new Concept of Semi-active Control of Truck's Suspension. Vehicle System Dynamics, 27, 289-303.

[38] Koo, J. H. (2003). Using Magneto-rheological Dampers in Semiactive Tuned Vibration Absorbers to Control Structural Vibrations. Doctoral Dissertation. Virginia Polytechnic Institute and State University.

[39] Ji, H. R., Moon, Y. J., Kim, C. H., & Lee, I. W. (2005, December). Structural Vibration Control Using Semiactive Tuned Mass Damper. 18th KKCNN Symposium on Civil Engineering, KAIST, Taiwan, 18-20.

[40] Setareh, M. (2001). Application of Semi-active Tuned Mass Dampers to Base-excited Systems. Earthquake Engineering & Structural Dynamics, 30(3), 449-462.

[41] Krasnicki EJ. (1980).The Experimental Performance of an On-Off Active Damper. 51th Shock and Vibration Symposium, San Diego, USA.

[42] Vamvatsikos, D., & Cornell, C. A. (2002). Incremental Dynamic Analysis. Earthquake Engineering & Structural Dynamics, 31(3), 491-514.

[43] Jalayer, F., & Cornell, C. A. (2009). Alternative Non-linear Demand Estimation Methods for Probability-based Seismic Assessments. Earthquake Engineering & Structural Dynamics, 38(8), 951-972.

[44] Cornell, C. A., Jalayer, F., Hamburger, R. O., & Foutch, D. A. (2009). Probabilistic Basis for 2000 SAC Federal Emergency Management Agency Steel Moment Frame Guidelines. Journal of structural engineering, 128(4), 526-533.

[45] Taylor, E. D. (2007). The Development of Fragility Relationships for Controlled Structures .Doctoral Dissertation. Washington University.

[46] American Society of Civil Engineers. (2000). Prestandard and Commentary for the Seismic Rehabilitation of Buildings. Federal Emergency Management Agency, Washington, D.C., USA.

[47] Azimi, S., Karami, K., & Nagarajaiah, S. (2021). Developing a Semi-active Adjustable Stiffness Device Using Integrated Damage Tracking and Adaptive Stiffness Mechanism. Engineering Structures, 238, Article e112036.

[48] Iervolino, I., & Cornell, C. A. (2005). Record Selection for Nonlinear Seismic Analysis of Structures. Earthquake Spectra, 21(3), 685-713.

[49] Kiani, J., Camp, C., & Pezeshk, S. (2018). On the Number of Required Response History Analyses. Bulletin of Earthquake Engineering, 16(11), 5195-5226.

[50] Jalayer, F., Ebrahimian, H., Miano, A., Manfredi, G., & Sezen, H. (2017). Analytical Fragility Assessment Using Unscaled Ground Motion Records. Earthquake Engineering & Structural Dynamics, 46(15), 2639-2663.